

# Deep Memory Update

Łukasz Neumann, Łukasz Lepak, Grzegorz Rypeś, Paweł Wawrzyński

Warsaw University of Technology  
Institute of Computer Science

Nowowiejska 15/19, 00-665 Warsaw, Poland

{lukasz.neumann|lukasz.lepak.dokt|grzegorz.rypesc.stud|pawel.wawrzynski}@pw.edu.pl

## Abstract

Recurrent neural networks are key tools for sequential data processing. However, they are notorious for problems regarding their training. Challenges include capturing complex relations between consecutive states and stability and efficiency of training. In this paper, we introduce a recurrent neural architecture called Deep Memory Update (DMU), as it is based on updating the previous memory state with a deep transformation of the lagged state and the network input. The architecture is able to learn the transformation of its internal state using an arbitrary nonlinear function. Its training is stable and relatively fast due to the speed of training varying according to a layer depth. Even though DMU is based on simple components, experimental results presented here confirm that it can compete with and often outperform state-of-the-art architectures such as Long Short-Term Memory, Gated Recurrent Units, and Recurrent Highway Networks.

## Introduction

Recurrent Neural Networks (RNNs) are designed to process sequential data and are key components of systems that perform speech recognition (Graves, Mohamed, and Hinton 2013), machine translation (Wu et al. 2016), handwritten text recognition (Capes et al. 2017), and other tasks (Schmidhuber 2015).

An intuitively designed RNN is prone to gradient explosions, or vanishing (Bengio, Simard, and Frasconi 1994) due to its recurrent nature. The impact of a given input on future outputs of the RNN may vanish or explode with time. Specialized architectures with gates, namely Long Short-Term Memory (LSTM) networks, (Hochreiter and Schmidhuber 1997) and Gated Recurrent Unit (GRU) networks (Cho et al. 2014a), are designed to overcome this problem at the level of a single neuron. While these networks are widely successful, they come with a cost — their memory state undergoes only single layer transformation from one time instant to another.

Several recurrent architectures apply deep processing of their internal states (Pascanu, Mikolov, and Bengio 2013; Chung et al. 2015; Zilly et al. 2017). However, they are complex and/or are difficult to train.

This paper addresses the above shortcomings by introducing a neural module designed to prevent the previously

mentioned gradient problems while allowing the state transformation to be modeled by an arbitrary feedforward neural network. We call this module Deep Memory Update (DMU). As a result, state transformation can easily be shaped in DMU. Additionally, the architecture is resistant to problems of gradient exploding/vanishing. Experimental results presented in the paper confirm that DMU performs well in comparison to its state-of-the-art counterparts.

## Related work

Early RNNs (Jordan 1986; Elman 1990; Robinson and Fallside 1987; Werbos 1988) suffered from the problem of gradient vanishing/exploding defined by Bengio, Simard, and Frasconi (1994): A small change in the RNN’s weights causes its future output’s change that is vanishing or exploding in time. As a result, the impact of RNN’s weights on its performance is either close to zero or infinity. In either case, it is impossible to train such a network. A gradient norm clipping strategy proposed in (Pascanu, Mikolov, and Bengio 2013) may mitigate this problem to some extent. (Arjovsky, Shah, and Bengio 2016) used orthogonal matrices of weights in shallow RNNs to stabilize the gradient successfully.

The gradient vanishing/exploding problem was alleviated at a cell level with Long Short-Term Memory (LSTM) networks (Hochreiter and Schmidhuber 1997). A neuron in such a network is a state machine with several so-called gates. The neuron generally preserves its state from one time to another but may also change it. The change depends on the dot product of the neuron inputs and its weights computed in its gates. LSTMs have been enhanced with batch normalization of recurrent signal (Cooijmans et al. 2017).

Cho et al. (2014a) proposed an architecture based on neurons simpler than those in LSTMs, called Gated Recurrent Units (GRUs). Despite its simplicity, it generally preserved the favorable properties of LSTM. Li et al. (2018) proposed a unit whose state was only computed based on its previous state and the outputs of the preceding neural layer. Networks based on such units, Independently Recurrent Neural Networks (IndRNNs), tend to outperform LSTMs and GRUs.

Capturing long-term dependencies in input sequences is a crucial challenge that RNNs face. Chang et al. (2017) proposed to increase lag of recurrent connections in higher network layers geometrically. Campos et al. (2018) introduced SkipRNN that learns to skip state updates and shorten the

effective size of the computational graph. Tallec and Ollivier (2018) prove that RNNs operate via transformations of time, and the gates in LSTM and GRU networks are a straightforward way to perform these transformations.

LSTMs and GRUs are usually organized in several layers stacked on top of one another (Graves 2013). Input to each neuron within a layer includes the previous states of all the neurons in the layer. This way, at each time instant, the network input undergoes a deep transformation. However, the internal state of the network undergoes only a shallow, single-layer transformation.

Being able to apply an arbitrary nonlinear, deep transformation to its internal state is a valuable feature of a recurrent neural network. Pascanu et al. (2014) proposed to increase the recurrence depth by adding multiple nonlinear layers to the recurrent transition, resulting in Deep Transition RNNs (DT-RNNs) and Deep Transition RNNs with Skip connections (DT(S)-RNNs). In these architectures, gradient propagation issues are exacerbated due to long credit assignment paths. Chung et al. (2015) added extra connections between all states across consecutive time steps in a stacked RNN, which also increases recurrence depth. However, their model requires extra connections with increasing depth, gives only a fraction of state cells access to the largest depth, and faces gradient propagation issues along the longest paths.

Zilly et al. (2017) introduced Recurrent Highway Networks (RHNs), which can be understood as LSTMs with specialized multilayer gates. These networks apply deep processing to their internal state while successfully coping with gradient vanishing/exploding.

A number of concepts may facilitate the performance of RNNs. Le, Jaitly, and Hinton (2015) proposed a scheme of initialization of weights in these networks. RNNs are usually trained with Stochastic Gradient Descent with gradient estimates computed with backpropagation through time. However, recent work of Kag and Saligrama (2021) on forward propagation through time calls this practice into question.

## Method

In this section, we introduce the Deep Memory Update (DMU) module. It is a neural module with memory designed to have the following properties:

1. Its memory state can undergo arbitrary nonlinear transformation from one moment to another.
2. The block can easily preserve its memory state from one moment of time to another.
3. Its learning is relatively fast and stable.

### General structure

We present the structure of the Deep Memory Update (DMU) module in Fig. 1. The module operates in discrete time  $t = 1, 2, \dots$ . At each time, the module is fed with the input  $x_t \in \mathbb{R}^n$  and produces the vector  $h_t \in \mathbb{R}^d$  which is both its memory state and its output.

A lagged memory state,  $h_{t-1}$ , together with an input of the block,  $x_t$ , are fed to a feedforward neural network (FNN). The network’s output layer is linear with  $2d$  neurons. It produces two vectors:  $z_t \in \mathbb{R}^d$  determines to what extent the

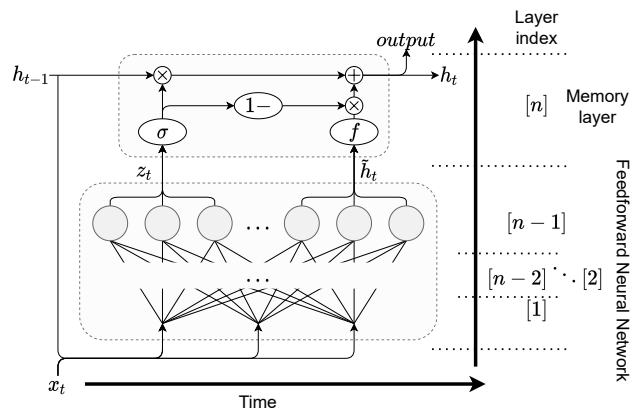


Figure 1: Structure of Deep Memory Update module. The module comprises of the feedforward neural network, which can arbitrarily process the state, and a memory layer. The output of the module is also its hidden state.

memory state should be preserved, and  $\tilde{h}_t \in \mathbb{R}^d$  determines the direction in which the state should change.

A pair of  $i$ -th elements of  $z_t$  and  $\tilde{h}_t$  are fed to a  $i$ -th memory cell. The cells update their state according to the formula

$$h_t = h_{t-1} \circ \sigma(z_t) + f(\tilde{h}_t) \circ (1 - \sigma(z_t)), \quad (1)$$

where “ $\circ$ ” denotes the elementwise product,  $\mathbf{1}$  is a vector of ones,  $\sigma$  is a unipolar soft step function, e.g. the logistic sigmoid,

$$\sigma_i(z) = \frac{e^{z_i}}{1 + e^{z_i}} \text{ for } z_i \in \mathbb{R},$$

and  $f$  is an activation function, e.g.

$$f_i(z) = \tanh(z_i) \text{ for } z_i \in \mathbb{R}.$$

Let us consider how the required properties of DMU are achieved.

1. Since a feedforward neural network with at least two dense layers is a universal function approximator, the network state can undergo the arbitrary nonlinear transformation from one time moment to another.
2. The block preserves its memory state for large values of  $z_t$ . In particular, for  $z_t = +\infty$  we have  $h_t = h_{t-1}$ .
3. For efficient and stable training of the network, it is enough that the speed of learning decreases with growing depth in the feedforward module, as discussed in a section below.

### Initialization

The FNN block should be a universal approximator. It can be a multilayer perceptron with at least two layers, including a linear output layer. This layer needs to be linear because its output should not be limited. It should be possible that  $z_t \gg 1$  which causes the memory state to be preserved,  $h_t \cong h_{t-1}$ .

We recommend using the standard ways of initializing neural weights in the FNN block, with one exception. Namely, upon weights’ initialization, we recommend adding a positive scalar to the biases of the neurons that produce  $z_t$  values, e.g.,

3. With positive elements of  $z_t$ , the memory state of the DMU module will be, by default, largely preserved from one moment  $t$  to another.

### Training

Training of DMU may be based on gradient backpropagation through time and using the gradient with a method of stochastic optimization such as Stochastic Gradient Descent or ADAM (Kingma and Ba 2014). Each such method applies to each trained weight a learning rate which defines a speed of optimization along derivatives with respect to this weight. We recommend to apply to each  $i$ -th layer inside the feedforward block of DMU a learning rate inversely proportional to the layer’s depth (i.e., to  $n + 1 - i$  in Fig. 1).

The following rationale justifies the above recommendation. A learning rate for a specific weight should be smaller than the inverse of the second derivative of the loss function being optimized with respect to this weight (Kushner and Yin 2003). However, for the sake of the optimization speed, this learning rate should not be too much smaller than that inverse.

In order to get insight into the values of the second derivatives in various layers of the feedforward module, we analyze its model in the form

$$x^i = \psi(w^i x^{i-1}), \quad i = 1, \dots, n, \quad (2)$$

in which  $\psi$  represents an activation function,  $w^i$  is a scalar weight and  $x^i$  is a scalar layer output. We are interested how  $d^2 L(x^n)/d(w^i)^2$  depends on  $i$  for  $L$  being a certain loss function. We have

$$\frac{dL(x^n)}{dw^i} = L'(x^n) \frac{x^{i-1}}{w^{i-1}} \prod_{j=i}^n \psi'(w^j x^{j-1}) w^{j-1}.$$

Then,

$$\begin{aligned} \frac{d^2 L(x^n)}{d(w^i)^2} &= \frac{dL(x^n)}{dw^i} \left( \frac{L''(x^n)}{L'(x^n)} \frac{x^{i-1}}{w^{i-1}} \prod_{j=i}^n \psi'(w^j x^{j-1}) w^{j-1} \right. \\ &\quad \left. + \sum_{k=i}^n \frac{\psi''(w^k x^{k-1}) w^k}{\psi'(w^k x^{k-1})} \frac{x^{i-1}}{w^{i-1}} \prod_{j=i}^{k-1} \psi'(w^j x^{j-1}) w^{j-1} \right). \end{aligned}$$

Now suppose that the gradient  $dL(x^n)/dw^i$  has the same scale for different  $i$ -s, i.e. it does not explode nor vanish. Then the terms

$$\frac{x^{i-1}}{w^{i-1}} \prod_{j=i}^{k-1} \psi'(w^j x^{j-1}) w^{j-1}$$

have the same scale for each  $i, k$ . Suppose also that  $x^i$ -s have the same scale for all  $i$ -s. For typical activation function that means that also  $w^i$ -s have the same scale for all  $i$ . Therefore, the scale of  $d^2 L(x^n)/d(w^i)^2$  is proportional to

$$\frac{L''}{L'} + (n - i + 1) \frac{\psi'' w}{\psi'}. \quad (3)$$

We conservatively assume that  $L''/L'$  does not dominate the above term and assume that the second derivative grows proportionally to  $n - i + 1$ . Therefore, the learning rate for  $w^i$  is decreased proportionally to  $(n - i + 1)^{-1}$ , which ensures stable training. If in fact  $L''/L'$  does dominate (3), such learning rates only slightly slow the training down.

## Experimental study

To evaluate the DMU architecture, we test it on three synthetic problems and three modern problems based on real-life data. The synthetic problems are taken from (Hochreiter and Schmidhuber 1997), and are noisy sequences, adding, and temporal order. The modern data-based problems are polyphonic music modeling (Boulanger-Lewandowski, Bengio, and Vincent 2012), natural language modeling (Zaremba, Sutskever, and Vinyals 2014), and Spanish/German/Portuguese to English machine translation tasks (Tatoeba 2020; ManyThings 2020).

We compare our DMU module using shallow architectures with ordinary recurrent neural networks (RNNs), GRU, and LSTM in the synthetic problems. We also compare DMU in its deep version with RHN in the data-based problems. To make the comparison fair, we embed a recursive subnetwork within the same neural architecture. That subnetwork is a layer or a few layers of recurrent units or a DMU module.

The hyperparameters of the architecture and training are manually optimized in preliminary runs separately for all network types. We present architectures for each problem in Table 1 and Table 2. Corresponding hyperparameters can be found in the supplemental material. The recurrent subnetwork is characterized by the number of units in subsequent layers. For example, a GRU subnetwork with two layers of 10 and 20 neurons will be briefly denoted by (10, 20). A DMU block with two FNN layers of 10 and 20 neurons will be denoted by (10, 20, 10) to account for the layer of memory cells within the block. In the data-based problems we evaluate each module on varying depths. In all cases the compared architectures have matching numbers of parameters.

The data is split into training, validation, and testing set. On synthetic problems, training continues until the loss reaches a specified threshold ( $10^{-6}$ ) on the validation set or the training budget is depleted. The error is then registered on the testing set and presented here. We follow a similar procedure for real-life problems, except the training process is stopped once the optimizer reaches the final epoch. All metrics are calculated using the model from the epoch with the best metric score on the validation set.

For each modern task/model/depth combination we run the experiment five times and aggregate the results. Standard result aggregation, such as averaging loss over time, would not be interpretable in the synthetic tasks since training is often unstable in these experiments. Therefore, the results for each synthetic problem are presented for multiple thresholds of the loss value. For each threshold, we plot the number of experiment runs that have reached the threshold in or before the specific epoch. These thresholds allow us to assess how fast and how likely does the module converges to a specific loss value. Thus, we can gain an insight into the quality of the module. The faster the algorithm reaches a specific threshold, the better. Convergence to lower thresholds is also preferable.

### Adding problem

The first task will hence be called “Adding”. In this problem, the network should output the sum of two randomly selected elements in the sequence of numbers. Specifically,

experiment		RNN	LSTM	GRU	DMU
NoiseSeq	rc. blk <sup>1</sup>	(5, 5)	(2, 2)	(2, 3)	((5, 4))
	weights no.	595	880	687	573
Adding	rc. blk <sup>1</sup>	(5, 5)	(2, 2)	(3, 2)	((5, 5))
	weights no.	111	99	108	106
TempOrd	rc. blk <sup>1</sup>	(6, 6)	(2, 3)	(2, 4)	((5, 6))
	weights no.	236	212	208	203

Table 1: Architectures used the for the comparison of different neural modules in synthetic experiments.<sup>1</sup>Recurrent block.

experiment	depth	RHN	DMU	weights no.
PolyMusic	1	100	100	46.7K
	2	100	122	66.9K
	5	100	131	127K
	10	100	136	228K
NatLang	1	100	100	1.7M
	2	100	122	1.7M
	5	100	131	1.8M
	10	100	136	1.9M
Translation	1	200	200	27.8M/36.6M/24.5M
	2	200	340	28.0M/36.8M/24.7M
	5	200	300	28.4M/37.3M/25.2M
	10	200	300	29.2M/38.1M/26.0M

Table 2: Architectures used for the comparison of RHN and DMU. We report number of neurons in feedforward layers. The last layer of the DMU’s FNN on Translation task has always 200 neurons. For Translation task, weights’ number are provided for Spa2Eng, Ger2Eng, and Por2Eng, respectively.

the network is fed with two-dimensional vectors  $[a, b]$ , where  $a$  is randomly chosen from the interval  $[-1, 1]$ , and  $b \in \{-1, 0, 1\}$  is a marker:  $-1$  denotes the first and last element of the sequence, there are two pairs marked by 1, the rest are marked by 0. The task of the network is to output the sum of  $a$ -s accompanied by  $b$ -s equal to 1 at the end of the sequence. See (Hochreiter and Schmidhuber 1997, sec. 5.4) for details. Each network analyzed is composed of a recurrent block and a layer with softmax activation.

**Results.** We present the results for the adding problem in Fig. 2. We conclude that DMU significantly outperforms all other modules. RNN is not able to reach any threshold while GRU scores better than LSTM.

### Temporal order

The next task, referred to as “TempOrd”, evaluates network’s ability to model temporal ordering of data. The input and the output are both 8-dimensional. They represent one of 8 symbols by one-hot encoding. The input symbols are:  $E$  (start),  $B$  (end),  $X$  or  $Y$ .  $X$  or  $Y$  occur at time  $t_1, t_2, t_3$ . In all three of these occurrences the choice of  $X$  or  $Y$  is random, the rest of a sequence is filled with symbols  $a, b, c, d$  also selected at random. Sequence length is chosen randomly between 100 and 110.  $t_1, t_2, t_3$  are selected randomly for each sequence, respectively between 10-20, 33-43 and 66-76. The output desired at the end of a sequence is either  $Q, R, S, U, V, A, B, C$ , depending on the combination of symbols that has occurred at times  $t_1, t_2$  and  $t_3$ . See (Hochreiter and Schmidhuber 1997, sec. 5.6, Task 6b) for details. Each network analyzed is composed of a recurrent block and a layer with softmax activation.

**Results.** The results for the temporal ordering problem are depicted in Fig. 3. We note that DMU has faster convergence than GRU and maintains similar results for high thresholds (up to  $10^{-4}$ ). For lower thresholds, DMU outperforms GRU. LSTM reaches partial success on higher thresholds but fails for lower ones. Likewise, RNN fails for all thresholds without a single successful run.

### Noise-free and noisy sequences

Long time lag problems force networks to hold to the state for a long duration of time. To test the modules under such conditions, we use noisy sequences. We call this task “NoiseSeq”. The network is fed with symbols one-hot encoded in  $n$ -dimensional vectors. An input sequence is, with equal probability 0.5, either  $(x, a_1, \dots, a_{n-2})$  or  $(y, a_1, \dots, a_{n-2})$ , where  $x, y, a_1, \dots, a_{n-1}$  are selected on random prior to an experiment. The task of the network is to output the first symbol in the input sequence when at  $n - 1$ -st step. See (Hochreiter and Schmidhuber 1997, sec. 5.2) for details. Each analyzed neural network is composed of a recurrent block and a layer with softmax activation.

**Results.** Figure 4 contains the results for the NoiseSeq task. We observe that GRU and DMU obtain similar results with GRU training faster. Both of these architectures significantly outperform RNN and LSTM.

### Polyphonic music modeling

In this subsection, we evaluate modules on the polyphonic music modeling, referred to as “PolyMusic”. The task is based on the Nottingham music dataset (Boulanger-Lewandowski, Bengio, and Vincent 2012). Inputs and out-

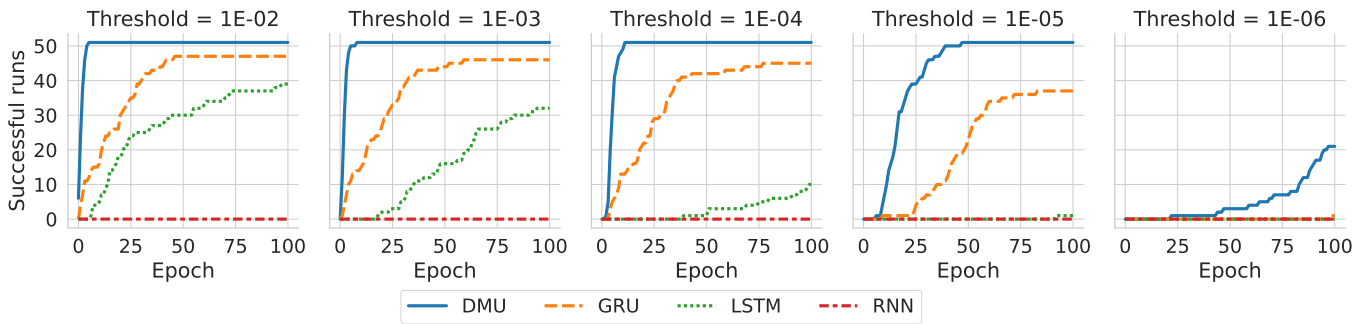


Figure 2: Adding: Results of 51 runs, 5 graphs for different loss thresholds.

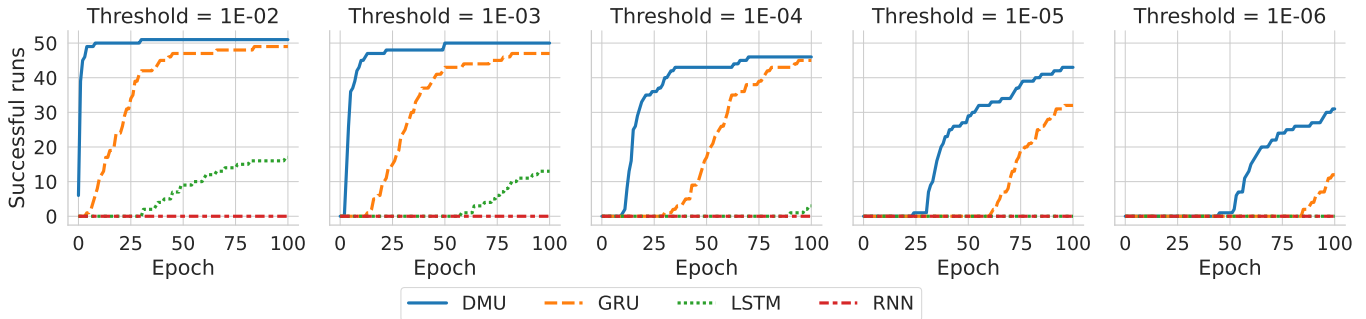


Figure 3: TempOrd: Results of 51 runs, 5 graphs for different loss thresholds.

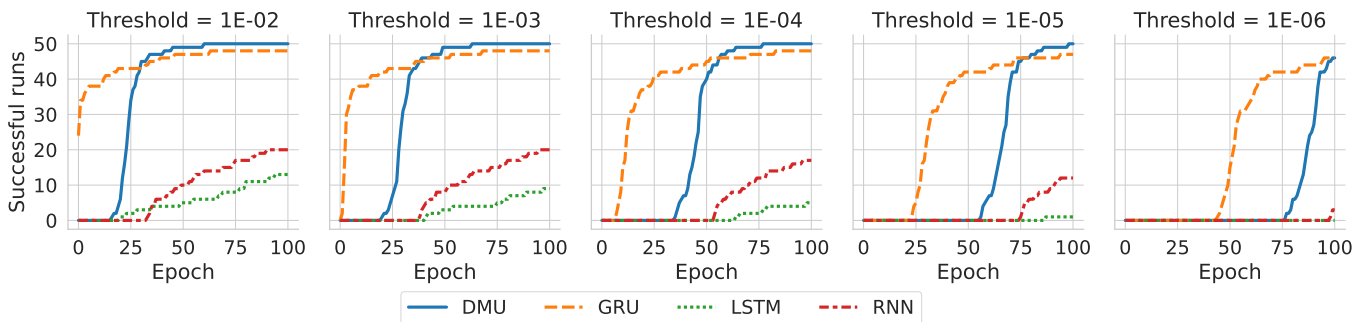


Figure 4: NoiseSeq: Results of 51 runs, 5 graphs for different loss thresholds.

puts are 88-dimensional. They represent the binary encoding of possible piano-rolls at a current timestep (in MIDI note numbers, between 21 and 108 inclusive). Sequences vary in length. The task of the model is to predict the next time step in the sequence (i.e., output at time  $t$  is equal to input at time  $t + 1$ ). The loss function is a negative log-likelihood averaged over all time steps in the dataset/batch. The neural network is composed of a recurrent block and a layer with the sigmoid activation.

**Results.** The results of the polyphonic music modeling can be found in Table 3. In this problem, DMU outperforms RHN at all depths with regard to all measures, with a single exception: RHN achieves better results for a depth of 10.

## Natural language modeling

The task, hence called “NatLang”, is based on the Penn Treebank corpus of English (Marcus, Santorini, and Marcinkiewicz 1993). Inputs and outputs are single number representations of the most frequent words in English and special tokens such as “unknown” or “end of sequence”. Sequences include 100 words. The goal of the network is to predict another word within the current sequence. The loss function is perplexity (categorical cross-entropy exponent). See (Zaremba, Sutskever, and Vinyals 2014) for details. The whole neural network comprises of a recurrent block, followed by a 100-neurons dense layer and an output layer with the softmax activation. For this experiment, the input word embedding is set to a small size (64) on purpose to limit overfitting.

depth	model	train			test		
		best	mean	std dev.	best	mean	std dev.
1	DMU	2.998	<b>2.966</b>	<b>0.038</b>	3.498	3.528	<b>0.025</b>
	RHN	3.344	3.375	0.078	3.552	3.598	0.037
2	DMU	<b>2.862</b>	3.008	0.125	<b>3.443</b>	<b>3.502</b>	0.056
	RHN	3.390	3.414	0.098	3.553	3.607	0.063
5	DMU	3.172	3.266	0.137	3.567	3.679	0.093
	RHN	3.443	3.682	0.163	3.734	3.851	0.106
10	DMU	3.356	3.538	0.140	3.960	4.155	0.158
	RHN	3.701	3.927	0.143	3.903	4.075	0.118

Table 3: PolyMusic: results — loss

**Results.** Table 4 shows the results of the experiments on natural language modeling dataset. DMU achieves slightly worse yet more stable results at each depth of both networks. There are however two exceptions: DMU achieves better average results for the largest depth. Also, the best average test result over all depths (at a depth of 1) is achieved by DMU.

### Machine translation

Finally, we test the modules in the context of machine translation, using complex architectures. The task is based on datasets of pairs of corresponding Spanish/Portuguese/German and English sentences (Tatoeba 2020; ManyThings 2020). We will call experiments based on subsequent pairs respectively “Spa2Eng”, “Por2Eng”, and “Ger2Eng”. In all languages, we use tokens representing words, punctuation marks, *sentence start*, and *sentence end*. Each token is encoded as a single, unique number. The goal is to translate Spanish/Portuguese/German sentences into English ones using a system with encoder-decoder architecture (Cho et al. 2014b,a; Sutskever, Vinyals, and Le 2014). A whole translator has encoder-decoder architecture. An encoder is a recurrent block. A decoder is composed of a recurrent block and a layer with the softmax activation. Additionally, we use input and output embeddings of size 650.

**Results.** Table 5 contains the results of machine translation experiments. DMU achieves better accuracy than RHN for all three language pairs at each depth of both networks. Additionally, both networks scores the best accuracy for a depth of 1 or 2. Accuracy generally deteriorates with growing depth, significantly faster for RHN than for DMU.

### Discussion

Since the seminal paper of Hochreiter and Schmidhuber (1997) the development of recurrent neural networks has been stimulated by the need to avoid gradient exploding or vanishing in backpropagation through time. Indeed, these phenomena are likely to occur in neural networks with feedback loops. In LSTM and GRU architectures, they were eliminated at the cell level.

The DMU neural module introduced in this paper is based on memory cells whose state is updated with the weighted average of their previous content and new values proposed for them. Both the weights and the new proposed values come

from a feedforward subnetwork whose inputs include the previous state of the memory cells. Architectures based on the DMU module compete and often outperform those based on LSTM or GRU. Although DMU is not equipped with any specific countermeasures against gradient vanishing/exploding, it never suffers from these phenomena.

In some applications, deep transformation of the network state is necessary. But then the effective length of gradient path increases, which may destabilize training. RHN successfully coped with this problem at the expense of the complexity of its architecture. DMU applies a typical feedforward block of any depth for state transformation. The stability of training is ensured by appropriately diversifying the speed of training in different layers. As a result, DMU performed better than RHN of the same depth in two out of three analyzed data-based problems.

Interestingly, contrary to Zilly et al. (2017) we note that depth-scaling of the model did not yield better results. We speculate that it can be explained by the lack of regularization other than weight decay. This was a deliberate choice to compare RHN and DMU modules without any unnecessary architectural additions.

### Conclusions

In this paper, we propose DMU — a recurrent neural module that is able to perform an arbitrary nonlinear transformation of its memory state. Three experiments with synthetic data (Adding, Temporal order, Noisy sequence) presented here compare neural architectures based on DMU with those based on RNN, LSTM, and GRU. Three experiments with real-life data (Polyphonic music, Natural language modeling, Machine translation) compare neural architectures based on DMU with those based on Recurrent Highway Network of the same depth. The architecture based on DMU outperformed the others in all cases, with the exception of Natural language modeling, in which RHN achieved a lower perplexity.

### References

- Arjovsky, M.; Shah, A.; and Bengio, Y. 2016. Unitary Evolution Recurrent Neural Networks. In *International Conference on Machine Learning (ICML)*, volume 48, 1120–1128.
- Bengio, Y.; Simard, P.; and Frasconi, P. 1994. Learning long-term dependencies with gradient descent is difficult. *IEEE transactions on neural networks*, 5(2): 157–166.

depth	model	train			test		
		best	mean	std dev.	best	mean	std dev.
1	DMU	65.983	67.045	<b>1.320</b>	107.371	<b>108.046</b>	<b>0.752</b>
	RHN	<b>61.102</b>	66.531	6.071	106.105	110.394	4.363
2	DMU	83.121	85.252	1.364	119.513	120.346	0.835
	RHN	62.895	<b>66.317</b>	4.232	<b>104.888</b>	109.833	4.040
5	DMU	93.755	99.964	3.971	128.823	133.251	2.810
	RHN	82.325	86.097	3.832	123.158	124.971	1.923
10	DMU	128.405	145.302	22.709	156.704	170.207	18.504
	RHN	85.972	149.430	86.869	124.458	171.598	60.383

Table 4: NatLang: results — perplexity

lang pair	depth	model	train			test			
			best	mean	std dev.	best	mean	std dev.	
Spa2Eng	1	DMU	0.908	0.906	0.015	<b>0.693</b>	<b>0.690</b>	0.003	
		RHN	0.893	0.909	0.012	0.688	0.684	0.003	
	2	DMU	<b>0.939</b>	<b>0.915</b>	0.027	0.683	0.681	<b>0.002</b>	
		RHN	0.911	0.908	0.011	0.686	0.680	0.003	
	5	DMU	0.772	0.764	<b>0.007</b>	0.631	0.627	0.005	
		RHN	0.761	0.680	0.059	0.574	0.549	0.021	
	10	DMU	0.652	0.647	0.022	0.588	0.574	0.016	
		RHN	0.304	0.275	0.017	0.306	0.283	0.012	
	Por2Eng	1	DMU	0.937	0.936	0.007	<b>0.776</b>	<b>0.773</b>	0.003
			RHN	0.937	0.935	<b>0.006</b>	0.776	0.768	0.005
2		DMU	<b>0.943</b>	<b>0.943</b>	0.008	0.768	0.765	<b>0.003</b>	
		RHN	0.928	0.932	0.008	0.769	0.761	0.005	
5		DMU	0.819	0.813	0.008	0.717	0.710	0.005	
		RHN	0.899	0.834	0.103	0.720	0.674	0.054	
10		DMU	0.741	0.715	0.017	0.669	0.652	0.012	
		RHN	0.396	0.312	0.042	0.380	0.310	0.035	
Ger2Eng		1	DMU	<b>0.931</b>	0.920	0.014	<b>0.749</b>	0.743	0.004
			RHN	0.915	0.920	0.008	0.746	<b>0.744</b>	<b>0.001</b>
	2	DMU	0.928	<b>0.926</b>	<b>0.005</b>	0.736	0.733	0.002	
		RHN	0.921	0.924	0.006	0.741	0.736	0.005	
	5	DMU	0.810	0.785	0.016	0.689	0.679	0.010	
		RHN	0.830	0.775	0.044	0.670	0.635	0.022	
	10	DMU	0.699	0.573	0.083	0.632	0.554	0.056	
		RHN	0.442	0.350	0.064	0.448	0.348	0.063	

Table 5: Translation: results — accuracy

Boulanger-Lewandowski, N.; Bengio, Y.; and Vincent, P. 2012. Modeling Temporal Dependencies in High-Dimensional Sequences: Application to Polyphonic Music Generation and Transcription. *Proceedings of the 29th International Conference on Machine Learning, ICML 2012*, 2.

Campos, V.; Jou, B.; i Nieto, X. G.; Torres, J.; and Chang, S.-F. 2018. Skip RNN: Learning to Skip State Updates in Recurrent Neural Networks. In *International Conference on Learning Representations (ICLR)*.

Capes, T.; Coles, P.; Conkie, A.; Golipour, L.; Hadjitarkhani, A.; Hu, Q.; Huddleston, N.; Hunt, M.; Li, J.; Neeracher, M.; and Prahallad, K. 2017. Siri On-Device Deep Learning-Guided Unit Selection Text-to-Speech System. In *Inter-speech*, 4011–4015.

Chang, S.; Zhang, Y.; Han, W.; Yu, M.; Guo, X.; Tan, W.; Cui, X.; Witbrock, M.; Hasegawa-Johnson, M.; and Huang,

T. S. 2017. Dilated Recurrent Neural Networks. In *Neural Information Processing Systems (NIPS)*.

Cho, K.; Merriënboer, B. V.; Gulcehre, C.; Bahdanau, D.; Bougares, F.; Schwenk, H.; and Bengio, Y. 2014a. Learning phrase representations using RNN encoder-decoder for statistical machine translation. In *Conference on Empirical Methods in Natural Language Processing (EMNLP2014)*.

Cho, K.; van Merriënboer, B.; Bahdanau, D.; and Bengio, Y. 2014b. On the Properties of Neural Machine Translation: Encoder-Decoder Approaches. ArXiv:1409.1259.

Chung, J.; Gulcehre, C.; Cho, K.; and Bengio, Y. 2015. Gated Feedback Recurrent Neural Networks. In *International Conference on Machine Learning (ICML)*, 2067–2075.

Cooijmans, T.; Ballas, N.; Laurent, C.; Çağlar Gülçehre; and Courville, A. 2017. Recurrent Batch Normalization. In *International Conference on Learning Representations (ICLR)*.

- Elman, J. L. 1990. Finding structure in time. *Cognitive science*, 14(2): 179–211.
- Graves, A. 2013. Generating sequences with recurrent neural networks. ArXiv:1308.0850.
- Graves, A.; Mohamed, A.; and Hinton, G. 2013. Speech Recognition with Deep Recurrent Neural Networks. ArXiv:1303.5778.
- Hochreiter, S.; and Schmidhuber, J. 1997. Long short-term memory. *Neural computation*, 9(8): 1735–1780.
- Jordan, M. I. 1986. Serial Order: A Parallel, Distributed Processing Approach. *Advances in Connectionist Theory Speech*, 121(ICS-8604): 471–495.
- Kag, A.; and Saligrama, V. 2021. Training Recurrent Neural Networks via Forward Propagation Through Time. In *International Conference on Machine Learning (ICML)*, 5189–5200.
- Kingma, D.; and Ba, J. 2014. Adam: A Method for Stochastic Optimization. *International Conference on Learning Representations (ICLR)*.
- Kushner, H.; and Yin, G. 2003. *Stochastic Approximation and Recursive Algorithms and Applications*. Springer.
- Le, Q. V.; Jaitly, N.; and Hinton, G. E. 2015. A Simple Way to Initialize Recurrent Networks of Rectified Linear Units. ArXiv:1504.00941.
- Li, S.; Li, W.; Cook, C.; Zhu, C.; and Gao, Y. 2018. Independently Recurrent Neural Network (IndRNN): Building a Longer and Deeper RNN. In *The IEEE Conference on Computer Vision and Pattern Recognition (CVPR)*.
- ManyThings. 2020. <http://www.manythings.org/anki/>. Retrieved 2020-05-05.
- Marcus, M.; Santorini, B.; and Marcinkiewicz, M. A. 1993. Building a large annotated corpus of English: The Penn Treebank. *Computational Linguistics*, 19(2): 313–330.
- Pascanu, R.; Gulcehre, C.; Cho, K.; and Bengio, Y. 2014. How to Construct Deep Recurrent Neural Networks. In *International Conference on Learning Representations (ICLR)*.
- Pascanu, R.; Mikolov, T.; and Bengio, Y. 2013. On the difficulty of training recurrent neural networks. In *International Conference on Machine Learning (ICML)*, 1310–1318.
- Robinson, A. J.; and Fallside, F. 1987. The utility driven dynamic error propagation network. Technical Report CUED/F-INFENG/TR.1, Cambridge University, Engineering Department.
- Schmidhuber, J. 2015. Deep learning in neural networks: An overview. *Neural networks*, 61: 85–117.
- Sutskever, I.; Vinyals, O.; and Le, Q. V. 2014. Sequence to Sequence Learning with Neural Networks. ArXiv:1409.3215.
- Tallic, C.; and Ollivier, Y. 2018. Can recurrent neural networks warp time? In *International Conference on Learning Representations (ICLR)*.
- Tatoeba. 2020. <https://tatoeba.org>. Retrieved 2020-05-05.
- Werbos, P. J. 1988. Generalization of backpropagation with application to a recurrent gas market model. *Neural Networks*, 1(4): 339–356.
- Wu, Y.; Schuster, M.; Chen, Z.; Le, Q.; Quoc, V.; Norouzi, M.; Macherey, W.; Krikun, M.; Cao, Y.; and Gao, Q. 2016. Google’s Neural Machine Translation System: Bridging the Gap between Human and Machine Translation. ArXiv:1609.08144.
- Zaremba, W.; Sutskever, I.; and Vinyals, O. 2014. Recurrent neural network regularization. ArXiv:1409.2329.
- Zilly, J. G.; Srivastava, R. K.; Koutník, J.; and Schmidhuber, J. 2017. Recurrent Highway Networks. In *International Conference on Machine Learning (ICML)*.

## Hyperparameter settings

Hyperparameters used for each experiment/neural module are presented in Table 6 and Table 7.

## Hardware

Our experiments have been performed on a PC equipped with AMD™Ryzen 1920X, 64GB RAM, 4xNVidia™RTX 2070 Super.

## Testing strategy

To evaluate synthetic tasks, we run an experiment for each module 51 times and aggregate the results. On real-life data tasks, we aggregate results over five runs for each recurrent module. We report metrics obtained in the `best` runs. These runs are selected based solely on their performance on the test set. Therefore, in some cases, metrics reported in the `best` column for the training dataset are worse than those in the `mean` column.



experiment	hyperparameter	RNN	LSTM	GRU	DMU
NoiseSeq	learning rate	0.01	0.002	0.1	0.02
	sequences per epoch	200	200	200	200
	min sequence length	100	100	100	100
	max epochs	100	100	100	100
Adding	learning rate	0.01	0.001	0.05	0.02
	sequences per epoch	200	200	200	200
	min sequence length	100	100	100	100
	max epochs	100	100	100	100
TempOrd	learning rate	0.01	0.005	0.02	0.05
	sequences per epoch	200	200	200	200
	min sequence length	100	100	100	100
	max epochs	100	100	100	100

Table 6: Hyperparameters used for synthetic tasks.

experiment	depth	hyperparameter	RHN	DMU
PolyMusic	all	max epochs	500	500
	1	learning rate	0.005	0.005
		weight decay	0.001	0.0001
		scheduler gamma	1.0	1.0
	2	learning rate	0.005	0.005
		weight decay	0.001	0.0001
		scheduler gamma	1.0	1.0
	5	learning rate	0.005	0.005
		weight decay	0.001	0.0001
		scheduler gamma	1.0	1.0
	10	learning rate	0.005	0.002
		weight decay	0.001	0.0001
scheduler gamma		1.0	1.0	
NatLang	all	max epochs	40	40
	1	learning rate	0.02	0.02
		weight decay	0.0001	0.0001
		scheduler gamma	0.9	0.8
	2	learning rate	0.02	0.002
		weight decay	0.0001	0.0001
		scheduler gamma	0.9	1.0
	5	learning rate	0.02	0.002
		weight decay	0.0001	0.0001
		scheduler gamma	0.9	1.0
	10	learning rate	0.02	0.002
		weight decay	0.0001	0.0001
scheduler gamma		0.9	1.0	
Spa2Eng/Por2Eng/Deu2Eng	all	teacher forcing ratio	1.0	1.0
		max epochs	50	50
	1	learning rate	0.01	0.005
		weight decay	0.0001	0.0001
		scheduler gamma	0.9	0.9
	2	learning rate	0.01	0.01
		weight decay	0.0001	0.0001
		scheduler gamma	0.9	0.9
	5	learning rate	0.01	0.003
		weight decay	0.0001	0.0001
		scheduler gamma	0.9	1.0
	10	learning rate	0.01	0.003
weight decay		0.0001	0.0001	
scheduler gamma		0.9	1.0	

Table 7: Hyperparameters used for each experiment and each neural module.